# Hyperpolarized 1 H and 13 C NMR spectroscopy in a single experiment for metabolomics

Arnab Dey, Benoît Charrier, Victor Ribay, Jean-Nicolas Dumez, Patrick Giraudeau

# Hyperpolarized $^{1}H$ and $^{13}C$ NMR spectroscopy in a single experiment for metabolomics

Arnab Dey*†, Benoît Charrier, Victor Ribay, Jean-Nicolas Dumez, Patrick Giraudeau*

Nantes Université, CEISAM UMR 6230, 44000, Nantes, France

**ABSTRACT:** The application of NMR spectroscopy to complex mixture analysis, and in particular to metabolomics, is limited by the low sensitivity of NMR. We recently showed that dissolution Dynamic Nuclear Polarization (d-DNP) could enhance the sensitivity of $^{13}C$ NMR for complex metabolite mixtures, leading to the detection of highly sensitive $^{13}C$ NMR fingerprints of complex samples such as plant extracts or urine. While such experiments provide heteronuclear spectra, which are complementary to conventional NMR, hyperpolarized $^{1}H$ NMR spectra would also be highly useful, with improved limits of detection and compatibility with existing metabolomics workflow and databases. In this technical note, we introduce an approach capable of recording both $^{1}H$ and $^{13}C$ hyperpolarized spectra of metabolite mixtures in a single experiment and on the same hyperpolarized sample. We investigate the analytical performance of this method in terms of sensitivity and repeatability, then we show that it can be efficiently applied to a plant extract. Significant sensitivity enhancements in $^{1}H$ NMR are reported with a repeatability suitable for metabolomics studies, without compromising on the performance of hyperpolarized $^{13}C$ NMR. This approach provides a way to perform both $^{1}H$ and $^{13}C$ hyperpolarized NMR metabolomics with unprecedented sensitivity and throughput.

Nuclear Magnetic Resonance spectroscopy (NMR) is a major analytical tool for the quantitative and structural analysis of complex mixtures, thanks to its high accuracy and robustness[1]. NMR spectroscopy is therefore widely used in bioanalytical applications such as metabolomics which impacts several scientific areas such as clinical and preclinical studies[2], microbiology[3], forensics[4], and food[5] and plant sciences[5]. On the one hand, the majority of NMR metabolomics studies rely on 1D $^{1}H$ NMR spectroscopy thanks to its high sensitivity compared to other nuclei. However, the analysis of complex mixtures by 1D $^{1}H$ spectroscopy is hampered by ubiquitous overlap between peaks. On the other hand, $^{13}C$ NMR offers a much better separation between peaks, but it suffers from a 2900-fold reduced sensitivity at natural abundance compared to $^{1}H$ NMR (owing to its low natural abundance and low gyromagnetic ratio).

Recent developments of hyperpolarization techniques in $^{13}C$ NMR have broadened the scope of NMR metabolomic studies by considerably improving sensitivity while retaining the spectral resolution advantages of $^{13}C$ NMR[6–15]. Dissolution Dynamic Nuclear Polarization (d-DNP) is particularly promising for $^{13}C$ NMR spectroscopy of complex metabolic mixtures, as it can improve signal sensitivity by more than 10,000 for $^{13}C$ nuclei with long longitudinal relaxation times[16]. In d-DNP, nuclear spins are polarized in the solid-state at cryogenic temperatures (typically 1-2 K), in a high magnetic field (3-7 T), by microwave irradiation in the presence of a free radical. This is followed by rapid dissolution and transfer of the sample to a nearby NMR spectrometer where hyperpolarized signals are acquired in the liquid-state. Since the inception of d-DNP, significant progress has been made to obtain improved throughput, precise and robust data that are essential for metabolomics studies. d-DNP enhanced stable-isotope resolved metabolomic studies were reported by quantifying the $^{13}C$ isotopic patterns to understand the metabolic activity of cancer cell extracts incubated with $^{13}C$-enriched glucose [17–19]. Recent investigations also focused on the development of d-DNP methods to analyze metabolic samples at natural $^{13}C$ abundance, taking advantage of $^{1}H \rightarrow {}^{13}C$ cross polarization (CP) in the solid-state to reach high $^{13}C$ polarization levels in a short time[20,21]. In 2015, we showed that d-DNP could be used to detect metabolites of plant and cell extracts at $^{13}C$ natural abundance.[8] The suitability of d-DNP for metabolomics applications was further strengthen by reporting the good repeatability of this approach[6]. The first proof-of-concept application of a d-DNP based $^{13}C$ metabolomics workflow at natural abundance was then successfully reported on model plant extracts[7]. Recently, a fine optimization of the d-DNP setting provided a significant sensitivity improvement (about 5 times improvement on quaternary $^{13}C$ and 50 times improvement on protonated $^{13}C$) with an excellent repeatability (in the range of 3%)[22]. This optimization enabled the acquisition of hyperpolarized $^{13}C$ spectra of freeze-dried urine at natural abundance, allowing the quantification of key metabolites that were difficult to access with conventional NMR[23].

While hyperpolarized $^{13}C$ NMR spectra are highly valuable, hyperpolarized $^{1}H$ NMR spectra would also be of high interest for complex mixture analysis, since i/ they can

provide improved limits of detection; ii/ extensive workflows and databases are available for their analysis. Hyperpolarized $^{13}C$ and $^{1}H$ NMR are thus expected to be highly complementary. The detection of hyperpolarized $^{1}H$ signals with d-DNP is challenging, since the shorter longitudinal relaxation times ($T_1$) of $^{1}H$ nuclei make the corresponding hyperpolarization short-lived and less likely to survive transfer between the two magnets. Recent developments to shorten the transfer time and/or extend the lifetime of $^{1}H$ hyperpolarization have enabled the acquisition of hyperpolarized $^{1}H$ spectra,[24,25] but these have not been applied to metabolite mixtures, neither evaluated from an analytical point of view. In addition, classic d-DNP strategies rely on the polarization of a single class of nuclei, and this would mean that separate sets of dissolution are needed to obtain both $^{1}H$ and $^{13}C$ NMR data.

In this article, we show that both hyperpolarized $^{13}C$ and $^{1}H$ NMR spectra can be recorded within a single experiment to maximize the spectral information that can be retrieved from a single sample. This is made possible by multiple receiver channels available on modern spectrometers. Parallel acquisitions on multiple nuclei have been extensively demonstrated on small molecule examples, including the parallel acquisition of multi-dimensional spectra on metabolite mixtures[26,27]. The parallel acquisition of $^{1}H$ and $^{13}C$ relaxation data after d-DNP was also reported[28,29]. In this study, we show how this concept can be adapted to maximize the spectral information that can be retrieved from a single d-DNP experiment, by sequentially recording $^{1}H$ and $^{13}C$-{$^{1}H$} spectra on a single hyperpolarized metabolite mixture. The repeatability of this experiment -a key feature for metabolomics applications- is demonstrated, as well as its feasibility on a real biological extract.

## Experimental section

### d-DNP operational procedure

d-DNP experiments were carried out with a semi-automated d-DNP workflow in which samples were polarized in a prototype Bruker d-DNP Polarizer of 7.05 T and at the temperature of 1.15 K with frequency-modulated, gated microwave. The operational timeline and the simplified pulse diagram are presented in Figure 1. $^{1}H$ spins were hyperpolarized directly from microwave(MW)-irradiated electrons of the TEMPOL radical and $^{13}C$ spins were hyperpolarized using cross-polarization (CP) to reach high $^{13}C$ polarization levels in about 20 minutes[30,31]. In the cross-polarization (CP) experiment, a train (k=64) of $\pi/2$ pulses was applied to both RF channels for pre-saturation. Then the adiabatic half passage pulses ($t_w$ = 175 µs) were applied before and after the ~~the~~ contact pulse ($t_{HH}$ = 1.5 ms). In total 16 CP contacts (n=16) were made and for each contact, a low-flip-angle pulse (5°) was applied on the $^{13}C$ channel to monitor the build-up of the polarization from $^{1}H$ to $^{13}C$. Microwave irradiation was selectively switched on after each CP contact for 80 s.[20,21,32] All the parameters involved in the DNP experiment were optimized as described in our previous study[22]. After hyperpolarization, 5 mL of hot solvent ($D_2O$ and/ or $CD_3OD$) were used to rapidly dissolve the sample and bring it to the nearby liquid-state spectrometer through a transfer line equipped with a 0.56 T magnetic tunnel. The dissolution time depends on the choice of the dissolution solvents as indicated in Figure 1. $CD_3OD$ has a smaller viscosity and surface tension than $D_2O$, allowing a shorter transfer and stabilization delay. Further details on the d-DNP system including the choice of optimum dissolution delays may be found in a previous study[22].

### Signal acquisition

$^{1}H$ and $^{13}C$ signal acquisition were performed on a 400 MHz Bruker NEO spectrometer equipped with a direct-detection nitrogen cooled cryoprobe and double receiver channels at room temperature. The sequential acquisition pulse sequence was suitably adapted for our d-DNP experiment from the available Bruker double receiver pulse sequence library. Such acquisition pulse sequence enables minimal delay (20 µs) between the completion of $^{1}H$ acquisition and the start of the $^{13}C$ read pulse. After an optimized stabilization delay, the sequential acquisition pulse sequence automatically triggered the $^{1}H$ signal acquisition with a 90° excitation pulse followed by the $^{13}C$ acquisition using a 90° excitation pulse on $^{13}C$ with a $^{1}H$ decoupling scheme (WALTZ-65). The $^{1}H$ signal was recorded for 1.99 s ($t_{acqu}$ ($^{1}H$)) with a spectral width of 12 kHz and the $^{13}C$ signal was recorded with an acquisition time of 1.72 s ($t_{acqu}$ ($^{13}C$)). Apodization ($^{1}H$: lb = 0.5 Hz; $^{13}C$: lb = 1 Hz) and zero filling ($^{1}H$ and $^{13}C$: 131K) were applied prior to Fourier Transform. Phase and baseline were corrected automatically. Chemical shifts were calibrated on the TSP methyl group (0 ppm). the $^{1}H$ and $^{13}C$ signal areas were normalized to the methyl $^{1}H$ signal of TSP (0 ppm) and quaternary $^{13}C$ TSP signal (188.5 ppm) respectively. All the spectra were acquired in the same conditions and processed the same way.

### Standard Mixture of metabolites

To evaluate the instrumental repeatability, a standard metabolite mixture solution at natural abundance containing three metabolites at 5 mM each was prepared (alanine, sodium acetate, sodium pyruvate) in an optimized glassy matrix of $H_2O/D_2O$/glycerol-$d_8$ (1:3:6) doped with 50 mM TEMPOL (4-hydroxy-2,2,6,6-tetramethylpiperidin-1-oxyl). Sodium 3-trimethylsilylpropionate-$d_4$ (Na-TSP-$d_4$; 98% D; 20 mM) was added as an internal standard, as previously reported[31]. For each dissolution experiment, 200 µL of the standard solution were transferred to the sample holder (the same being used for all experiments) from the same stock solution to avoid unwanted variation from the differences in sample measurement.

### Tomato Extract Preparation for d-DNP

A green tomato extract from a previous study[7] was used. The detailed description of the tomato extract preparation is given in that study[7]. The green tomato extract (20 mg) was dissolved with 2 mM of EDTA.$Na_2$.$2H_2O$, 20 mM Na-TSP-$d_4$ (internal reference) in 0.2 mL of a $H_2O/D_2O$/glycerol-$d_8$ (1:3:6) glass-forming mixture doped with 50 mM TEMPOL. After proper mixing, and ripening[22] for 30 mins, the resulting single-sample solution (approx. 200 µL) was transferred to the sample holder ensuring the solutions were contained within the active volume of radio frequency (RF) coil of the polarizer.

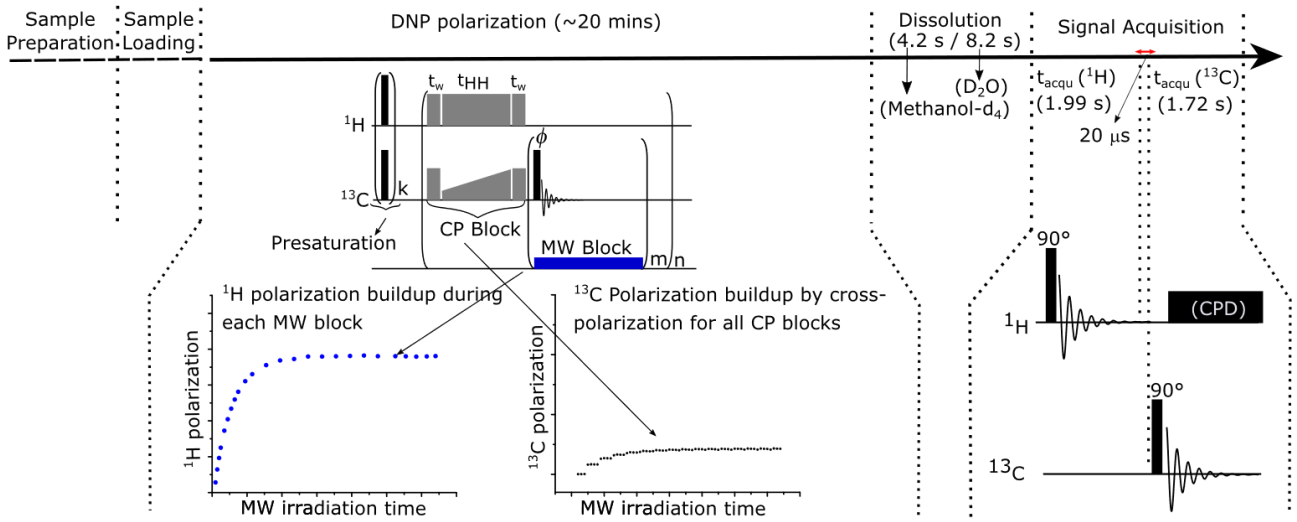


Figure 1. Operational timeline and pulse diagrams of the d-DNP experiment. In the cross-polarization (CP) pulse diagram, a train (k=64) of π/2 pulses was applied to both RF channels for pre-saturation. Here CP pulses (referred as "CP block" in grey) consisting of adiabatic half passage pulses ($t_w$ = 175 µs) were applied before the start of the contact pulse ($t_{HH}$ = 1.5 ms) and after the contact. In total 16 CP contacts (n=16) were made. For each contact, a sequence of m=4 low-flip-angle pulses (5°) was applied on the $^{13}C$ channel to monitor the build-up of the polarization from $^{1}H$ to $^{13}C$. Microwave irradiation was selectively switched on after each CP contact for 80 s ("MW block" in blue). After dissolution, the sequential acquisition pulse sequence automatically triggered the $^{1}H$ signal acquisition with 90° excitation pulse followed by the $^{13}C$ signal using 90° excitation pulse on $^{13}C$ with a $^{1}H$ decoupling scheme (WALTZ-65). The delay between the $^{1}H$ acquisition and $^{13}C$ read pulse was 20 µs (indicated with a red coloured double headed arrow).

## Results and discussion

### $^{1}H$ and $^{13}C$ spectra from a single hyperpolarized sample

Figure 2 presents the $^{1}H$ and $^{13}C$ spectra obtained (following the operational timeline as in Figure 1) from a single hyperpolarized metabolite mixture. Spectra show $^{1}H$ signal enhancements of metabolites in the 150-1800 range, as well as a high $^{13}C$ signal sensitivity (except alanine which constantly reported exceptionally poor $^{1}H$ polarization and poor $^{13}C$ sensitivity, as observed in previous studies[22]). In this study, SNR (signal to noise ratio) values were used as a measure of sensitivity. The liquid-state $^{1}H$ enhancements were calculated by comparing the hyperpolarized signal SNR with thermal SNR on spectra recorded in 128 scans on the same sample, 30 min after dissolution. The liquid-state $^{13}C$ enhancements were determined by comparing the single scan thermal signal integral of a higher concentrated metabolite sample (500 mM each) with the single scan hyperpolarized signal of the metabolite mixture. Spectra are shown with two different dissolution solvents ($D_2O$, $CD_3OD$). Indeed, we recently reported that both solvents offered a great complementarity, with dissolution parameters that could be tuned on a sample-dependent basis[22]. Here, the sample stabilization delay (relax time) was tuned to obtain optimum sensitivity and lineshape for each solvent (relax time = 6 s for $D_2O$ and 2 s for $CD_3OD$). Figure 2 shows that under such optimized conditions, the $^{1}H$ signal enhancement is an order of magnitude higher after dissolution in $CD_3OD$ compared to $D_2O$ (see also Figure S1 for SNR comparison). This can be attributed to the reduced hyperpolarization losses when a shorter stabilization delay is used and to the stronger impact of residual sample motion with the likely presence of (micro-)bubbles in $D_2O$, leading to *ca*. 3x broader line shapes compared to $CD_3OD$. Based on the hyperpolarized $^{1}H$ signal sensitivity (average SNR of metabolites is 550 with $D_2O$ and 3000 with $CD_3OD$) and on the metabolite concentrations (5 mM in the sample cup and *ca*. 0.05 mM after dissolution), one can extrapolate limits of detection (SNR>10) in the range of 50 µM in the sample cup for $^{1}H$ spectra recorded in methanol. In contrast to the $^{1}H$ signal, a slightly higher sensitivity (in the range of 20-150) was observed for $^{13}C$ spectra of metabolites recorded in $D_2O$ compared to $CD_3OD$. The $^{13}C$ enhancements reported here are in agreement with a previous report[22]. In the case of $^{13}C$ NMR, the difference in the delay between detection and dissolution between the two solvents is not significant with respect to the long $T_1$ of quaternary carbons, and the line shapes are much less impacted by residual sample motion. The sensitivity difference in favor of $D_2O$ can be explained by the higher solubility of metabolites in this solvent.

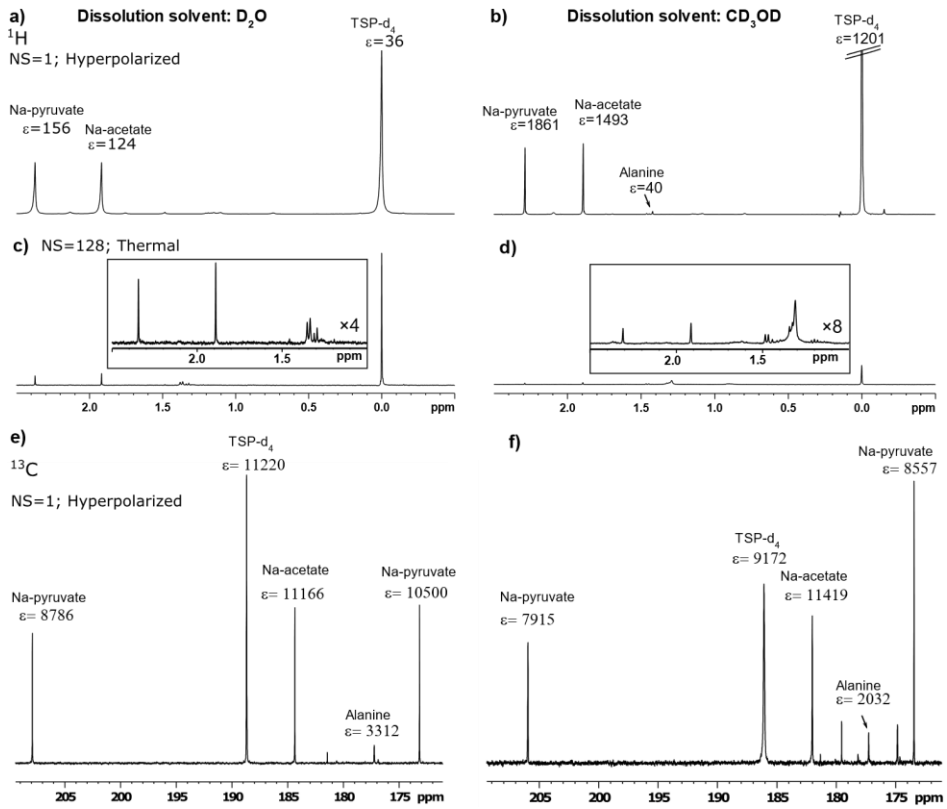


Figure 2. Spectra of a 5 mM metabolite mixture obtained from a single d-DNP experiment. Hyperpolarized $^{1}H$ spectra after dissolution in $D_2O$ (a) and in $CD_3OD$ (b) compared to spectra at thermal condition (ns= 128) in $D_2O$ (c) and $CD_3OD$ (d). The hyperpolarized $^{13}C$ spectra recorded after dissolution in $D_2O$ (e) and in $CD_3OD$ (f) are presented as well. $^{13}C$ thermal spectra could not be detected here due to the insufficient sensitivity even after a long experiment time (> 3 hr). The signal enhancement (ε) is indicated for each peak of the hyperpolarized spectra, and was calculated as indicated in the results and discussion section. For (c) and (d), vertical zooms are provided with scaling factors as an inset.

Evaluation of repeatability

To evaluate the analytical performance of the method, the signal integral repeatability of each metabolite was calculated from the d-DNP experiments on 5 samples from the same stock solution. Figure 3 compares the average value of absolute $^{1}H$ and $^{13}C$ signal integrals of metabolites obtained with the two dissolution solvents. The $^{1}H$ signal comparison revealed higher signal integrals with $CD_3OD$ compared to $D_2O$. However, $^{13}C$ signal integrals with $D_2O$ were higher compared to $CD_3OD$. This observation agrees with the sensitivity comparison discussed in the previous section. Note that additional T1 measurements (data not shown) excluded the impact of solvent dependent relaxation in that case. Overall, the absolute signal integral and SNR (figure S1) of both $^{13}C$ and $^{1}H$ spectra, particularly with $D_2O$, showed high variability (in between ~ 26% to 62%). Such variability may be attributed to the visual observation that microbubbles occur in $D_2O$ during sample transfer and injection, causing irregular flow and leading to variations in the final sample volume of the NMR tube. As previously suggested in the case of hyperpolarized $^{13}C$ metabolomics[7], such challenge can be addressed by normalizing the metabolite signal with the reference signal (TSP) (See SI; table 1 and 2). Normalized $^{1}H$ and $^{13}C$ signal integral (Tables SI1 and SI2) show good repeatability (between 3% to 11%) with both dissolution solvents. The repeatability of $^{13}C$ integrals is in line with previously reported results[22], and the repeatability of both spectra appears suitable for typical metabolomics applications. The repeatability of SNR values is given for information but is a less relevant metric than the repeatability of integral values for metabolomics applications.

Demonstration on a biological extract

The d-DNP enhanced $^{1}H$-$^{13}C$ sequential acquisition scheme was applied to record the $^{1}H$ and $^{13}C$ spectra of a green tomato extract, already used as a model biological sample in recent studies. Figure 4 presents the single-scan DNP enhanced $^{1}H$ spectra of the green tomato extract with both dissolution solvents. When comparing the two dissolution solvents, the DNP enhanced $^{1}H$ spectra with $CD_3OD$ provided much sharper and more sensitive signals compared to $D_2O$, resulting in a rich and well resolved $^{1}H$ fingerprint. The linewidth obtained in $CD_3OD$ is close to the one of typical liquid-state spectra in such extracts, *ie.* 2 Hz versus 10 Hz for $D_2O$. These results, in line with those obtained on the model mixture, are clearly in favor of the use of $CD_3OD$ as a dissolution solvent to obtain exploitable hyperpolarized $^{1}H$ metabolomics spectra. It should be noted that the hyperpolarization was performed at a MW frequency corresponding to the negative EPR resonance, which results in a

"negative" signal enhancement. Therefore, a 180° phase shift between the "thermal" signal of the residual protonated methanol in the dissolution solvent and the hyperpolarized analyte signals in the solution state was observed. Such negative signal is not observed for dissolution in $D_2O$ since the hyperpolarized sample does contain 10 % of $H_2O$, whose hyperpolarized signal largely outweighs the thermal signal from residual protonated water in the dissolution solvent.

In contrast to the $^1H$ study, the d-DNP enhanced $^{13}C$ spectra of the tomato extract with $D_2O$ showed better sensitivity compared to $CD_3OD$ (Figure 5). As discussed before, d-DNP enhanced $^{13}C$ signals were less perturbed by the presence of the microbubbles and less impacted by the polarization decay rate due to longer relaxation time. Therefore, the quality of the d-DNP enhanced $^{13}C$ spectra essentially depends on the solubility of the metabolites in the dissolution solvent. This means that the choice of the optimum dissolution solvent for a given sample will depend on the analyzed matrix, and also on the user's need to record both $^1H$ and $^{13}C$ spectra or only $^{13}C$ spectra.

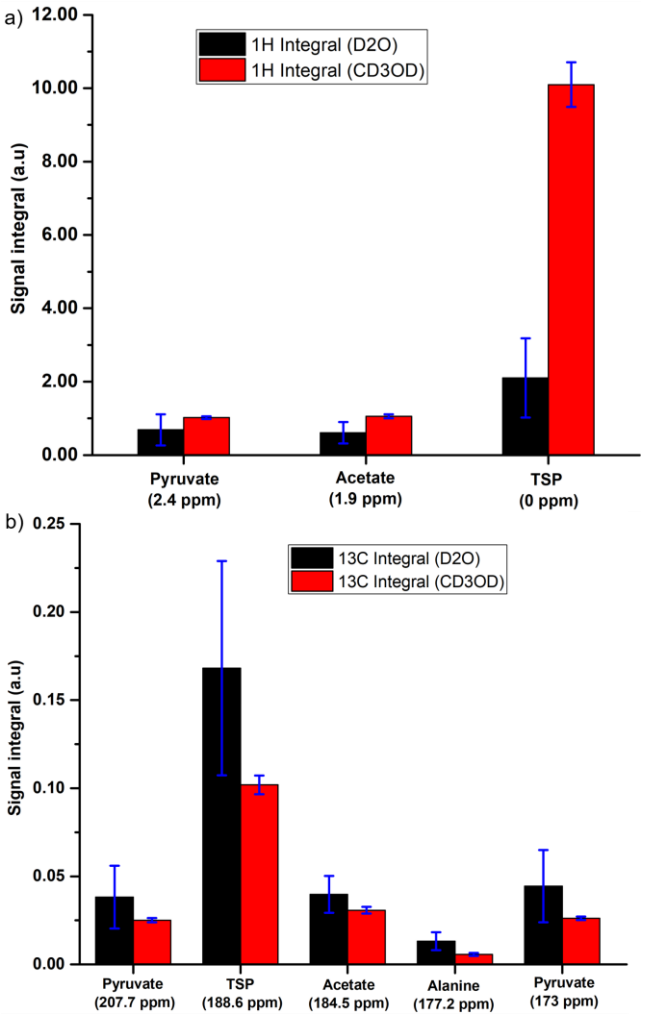


Figure 3. Comparison of absolute (a) $^1H$ and (b) $^{13}C$ signal integrals for hyperpolarized spectra of a model metabolic mixture after dissolution in two different solvents. The error bar represents the standard deviation of average signal integrals over 5 repetitions.

$^1H$ and $^{13}C$ hyperpolarized spectra of the tomato extract were also compared with conventional thermal spectra recorded on an extract from the same batch dissolved in 0.6 mL of $D_2O$, obtained in 5 min for $^1H$ and 1h 20min for $^{13}C$ spectra (see green spectra in Fig. 4 and 5). A detailed sensitivity comparison is beyond the scope of this study, but a clear trend is observed towards a much higher sensitivity of hyperpolarized spectra obtained in $CD_3OD$ for nuclei with sufficient typical $T_1$ values (*eg*., quaternary carbons, aromatic protons). On the contrary, the added value of d-DNP in the case of fast-relaxing nuclei (aliphatic protons in particular) is much less obvious. The aliphatic region of the hyperpolarized $^1H$ spectra is also hampered by signals from residual non-deuterated glycerol, pointing out towards the need to implement selective signal saturation strategies.

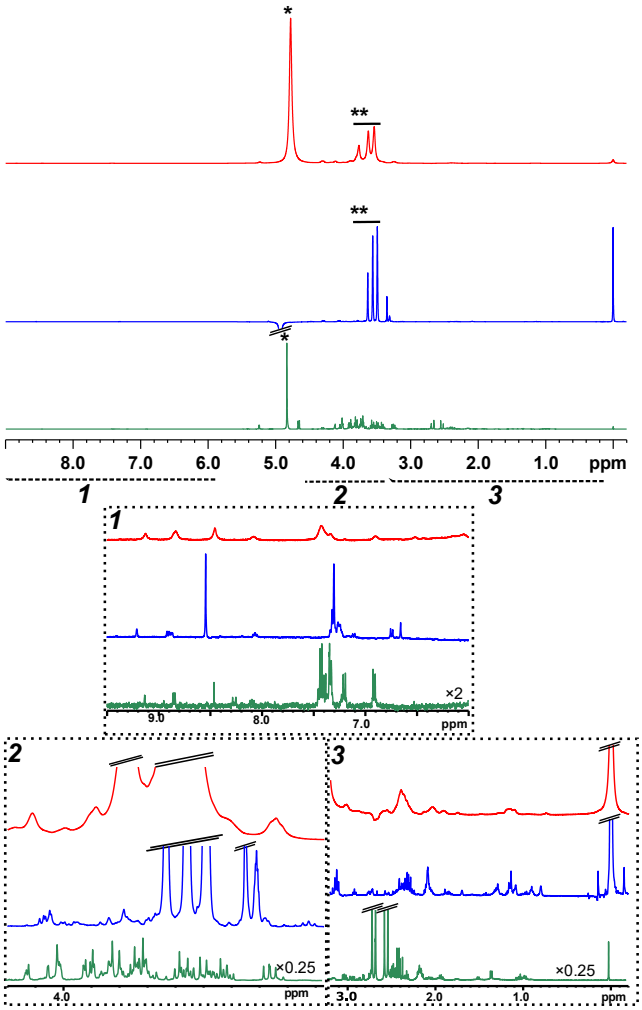


Figure 4. d-DNP hyperpolarized single scanned $^1H$ d-DNP signal of the Green tomato extract with two different dissolution solvents (Blue: with $CD_3OD$; Red: with $D_2O$) compared to the thermal spectrum in green, acquired on the same amount of extract dissolved in 0.6 mL of $D_2O$ (acquired no of scans=32 and experiment time ~ 5 min). Different regions of the spectra (indicated as 1, 2, 3) were enlarged at the bottom of the figure to highlight the metabolites signals and the thermal spectra were scaled as

indicated in the Figure for the sake of readability. The * marked peaks referred to the signals from the solvent and residual protonated glycerol.

### Conclusions

We demonstrated the possibility to record both hyperpolarized $^{1}H$ and $^{13}C$ spectra of complex metabolite mixtures, in a single experiment and at $^{13}C$ natural abundance. For $^{1}H$ hyperpolarized spectra, signal enhancements >$10^3$ were obtained, with a repeatability of a few percent that matches the requirements of metabolomics and a sub-millimolar limit of detection. For $^{13}C$ hyperpolarized spectra, the sensitivity and repeatability were in line with recently reported results where only $^{13}C$ spectra were recorded. This shows that $^{1}H$ hyperpolarized data can be accessed essentially for free, without significant penalty on hyperpolarized $^{13}C$ data. These results open application perspectives for metabolomic studies on a variety of samples and scientific questions. The performance of the method would benefit from ongoing developments that enable faster and less turbulent transfer between the polarizer and the NMR spectrometer[24,25]. In addition, the parallel acquisition of multi-nuclear 1D and single-scan 2D experiments could further extend the hyperpolarized metabolomics pulse sequence toolbox.

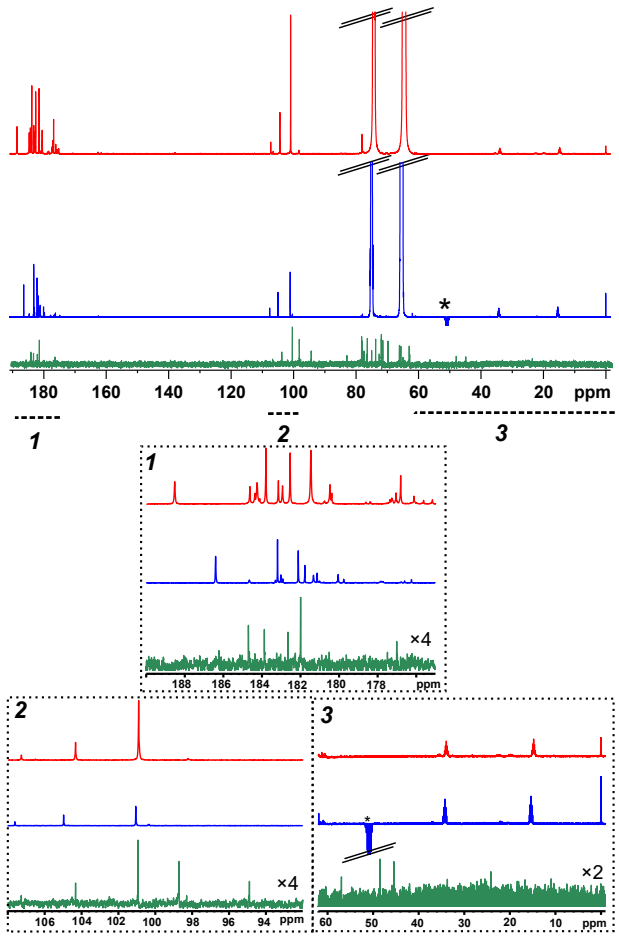


Figure 5. d-DNP hyperpolarized single scanned $^{13}C$ d-DNP signal of the Green tomato extract with two different dissolution solvents (Blue: with $CD_3OD$; Red: with $D_2O$) compared to the thermal spectrum in green, acquired on the same amount of extract dissolved in 0.6 mL of $D_2O$ (acquired no of scans=32 and experiment time ~ 5 min). Different regions of the spectra (indicated as 1, 2, 3) were enlarged at the bottom to highlight the metabolites signals and the thermal spectra were scaled as indicated in the Figure for the sake of readability. The * marked peaks referred to the signals from the residual protonated methanol in the dissolution solvent.

## ASSOCIATED CONTENT

### Supporting Information

The Supporting information contains two tables (table 1 and 2) showcasing the repeatability of $^{1}H$ and $^{13}C$ signals, and SNR comparison plots of $^{1}H$ and $^{13}C$ signals with two dissolution solvents.

## AUTHOR INFORMATION


### Corresponding Author

* E-mail: patrick.giraudeau@univ-nantes.fr, arnabd@ncbs.res.in

### Present Addresses

†National Centre for Biological Sciences, Tata Institute of Fundamental Research, GKVK Campus, Bellary Road, Bengaluru 560065, India


### Author Contributions

The manuscript was written through contributions of all authors. All authors have given approval to the final version of the manuscript.

## ACKNOWLEDGMENT


The authors are grateful to Dmitry Eshchenko, Marc Schnell, Roberto Melzi and James G. Kempf from Bruker Biospin for assembling and optimizing the d-DNP prototype. We would like to thank Sami Jannin's research group for valuable suggestions and support for the optimization of d-DNP setting. The authors acknowledge the help and guidence from Jerome Coutant from Bruker Biospin and Aurélie Bernard from CEISAM Lab for setting up the multireceiver NMR experiments. The authors acknowledge Catherine Deborde and Annick Moing for providing the tomato extract. This work has received funding from the European Research Council (ERC) under the European Union's Horizon 2020 research and innovation program (grant agreements no 814747/SUMMIT and 801774/DINAMIX) and the Region Pays de la Loire (ConnectTalent). The authors acknowledge the French National Infrastructure for Metabolomics and Fluxomics MetaboHUB-ANR-11-INBS-0010 (www.metabohub.fr) and the Corsaire metabolomics core facility (Biogenouest). This work includes NMR experiments carried out the on the CEISAM NMR platform.


## REFERENCES


(1) Bingol, K.; Brüschweiler, R. Two Elephants in the Room: New Hybrid Nuclear Magnetic Resonance and Mass Spectrometry Approaches for Metabolomics. *Curr. Opin. Clin. Nutr. Metab. Care* **2015**, *18* (5), 471–477. https://doi.org/10.1097/MCO.0000000000000206.

(2) Bizzarri, D.; Reinders, M. J. T.; Beekman, M.; Slagboom, P. E.; Bbmri-Nl; Van Den Akker, E. B. 1H-NMR Metabolomics-Based

Surrogates to Impute Common Clinical Risk Factors and Endpoints. *eBioMedicine* **2022**, *75*, 103764. https://doi.org/10.1016/j.ebiom.2021.103764.

(3) Palama, T. L.; Canard, I.; Rautureau, G. J. P.; Mirande, C.; Chatellier, S.; Elena-Herrmann, B. Identification of Bacterial Species by Untargeted NMR Spectroscopy of the Exo-Metabolome. *The Analyst* **2016**, *141* (15), 4558–4561. https://doi.org/10.1039/C6AN00393A.

(4) Castillo-Peinado, L. S.; Luque De Castro, M. D. Present and Foreseeable Future of Metabolomics in Forensic Analysis. *Anal. Chim. Acta* **2016**, *925*, 1–15. https://doi.org/10.1016/j.aca.2016.04.040.

(5) Petrakis, E. A.; Cagliani, L. R.; Polissiou, M. G.; Consonni, R. Evaluation of Saffron (Crocus Sativus L.) Adulteration with Plant Adulterants by 1H NMR Metabolite Fingerprinting. *Food Chem.* **2015**, *173*, 890–896. https://doi.org/10.1016/j.foodchem.2014.10.107.

(6) Bornet, A.; Maucourt, M.; Deborde, C.; Jacob, D.; Milani, J.; Vuichoud, B.; Ji, X.; Dumez, J.-N.; Moing, A.; Bodenhausen, G.; Jannin, S.; Giraudeau, P. Highly Repeatable Dissolution Dynamic Nuclear Polarization for Heteronuclear NMR Metabolomics. *Anal. Chem.* **2016**, *88* (12), 6179–6183. https://doi.org/10.1021/acs.analchem.6b01094.

(7) Dey, A.; Charrier, B.; Martineau, E.; Deborde, C.; Gandriau, E.; Moing, A.; Jacob, D.; Eshchenko, D.; Schnell, M.; Melzi, R.; Kurzbach, D.; Ceillier, M.; Chappuis, Q.; Cousin, S. F.; Kempf, J. G.; Jannin, S.; Dumez, J.-N.; Giraudeau, P. Hyperpolarized NMR Metabolomics at Natural $^{13}$ C Abundance. *Anal. Chem.* **2020**, *92* (22), 14867–14871. https://doi.org/10.1021/acs.analchem.0c03510.

(8) Dumez, J.-N.; Milani, J.; Vuichoud, B.; Bornet, A.; Lalande-Martin, J.; Tea, I.; Yon, M.; Maucourt, M.; Deborde, C.; Moing, A.; Frydman, L.; Bodenhausen, G.; Jannin, S.; Giraudeau, P. Hyperpolarized NMR of Plant and Cancer Cell Extracts at Natural Abundance. *The Analyst* **2015**, *140* (17), 5860–5863. https://doi.org/10.1039/C5AN01203A.

(9) Giraudeau, P.; Shrot, Y.; Frydman, L. Multiple Ultrafast, Broadband 2D NMR Spectra of Hyperpolarized Natural Products. *J. Am. Chem. Soc.* **2009**, *131* (39), 13902–13903. https://doi.org/10.1021/ja905096f.

(10) Guduff, L.; Kurzbach, D.; van Heijenoort, C.; Abergel, D.; Dumez, J.-N. Single-Scan $^{13}$ C Diffusion-Ordered NMR Spectroscopy of DNP-Hyperpolarised Substrates. *Chem. - Eur. J.* **2017**, *23* (66), 16722–16727. https://doi.org/10.1002/chem.201703300.

(11) Daniele, V.; Legrand, F.-X.; Berthault, P.; Dumez, J.-N.; Huber, G. Single-Scan Multidimensional NMR Analysis of Mixtures at Sub-Millimolar Concentrations by Using SABRE Hyperpolarization. *ChemPhysChem* **2015**, *16* (16), 3413–3417. https://doi.org/10.1002/cphc.201500535.

(12) Eshuis, N.; Hermkens, N.; Van Weerdenburg, B. J. A.; Feiters, M. C.; Rutjes, F. P. J. T.; Wijmenga, S. S.; Tessari, M. Toward Nanomolar Detection by NMR Through SABRE Hyperpolarization. *J. Am. Chem. Soc.* **2014**, *136* (7), 2695–2698. https://doi.org/10.1021/ja412994k.

(13) Singh, K.; Jacquemmoz, C.; Giraudeau, P.; Frydman, L.; Dumez, J.-N. Ultrafast 2D $^{1}$ H– $^{1}$ H NMR Spectroscopy of DNP-Hyperpolarised Substrates for the Analysis of Mixtures. *Chem. Commun.* **2021**, *57* (65), 8035–8038. https://doi.org/10.1039/D1CC03079E.

(14) Plainchont, B.; Berruyer, P.; Dumez, J.-N.; Jannin, S.; Giraudeau, P. Dynamic Nuclear Polarization Opens New Perspectives for NMR Spectroscopy in Analytical Chemistry. *Anal. Chem.* **2018**, *90* (6), 3639–3650. https://doi.org/10.1021/acs.analchem.7b05236.

(15) Lloyd, L. S.; Adams, R. W.; Bernstein, M.; Coombes, S.; Duckett, S. B.; Green, G. G. R.; Lewis, Richard. J.; Mewis, R. E.; Sleigh, C. J. Utilization of SABRE-Derived Hyperpolarization To Detect Low-Concentration Analytes via 1D and 2D NMR Methods. *J. Am. Chem. Soc.* **2012**, *134* (31), 12904–12907. https://doi.org/10.1021/ja3051052.

(16) Ardenkjær-Larsen, J. H.; Fridlund, B.; Gram, A.; Hansson, G.; Hansson, L.; Lerche, M. H.; Servin, R.; Thaning, M.; Golman, K. Increase in Signal-to-Noise Ratio of > 10,000 Times in Liquid-State NMR. *Proc. Natl. Acad. Sci.* **2003**, *100* (18), 10158–10163. https://doi.org/10.1073/pnas.1733835100.

(17) Frahm, A. B.; Jensen, P. R.; Ardenkjær-Larsen, J. H.; Yigit, D.; Lerche, M. H. Stable Isotope Resolved Metabolomics Classification of Prostate Cancer Cells Using Hyperpolarized NMR Data. *J. Magn. Reson.* **2020**, *316*, 106750. https://doi.org/10.1016/j.jmr.2020.106750.

(18) Lerche, M. H.; Yigit, D.; Frahm, A. B.; Ardenkjær-Larsen, J. H.; Malinowski, R. M.; Jensen, P. R. Stable Isotope-Resolved Analysis with Quantitative Dissolution Dynamic Nuclear Polarization. *Anal. Chem.* **2018**, *90* (1), 674–678. https://doi.org/10.1021/acs.analchem.7b02779.

(19) Frahm, A. B.; Hill, D.; Katsikis, S.; Andreassen, T.; Ardenkjær-Larsen, J. H.; Bathen, T. F.; Moestue, S. A.; Jensen, P. R.; Lerche, M. H. Classification and Biomarker Identification of Prostate Tissue from TRAMP Mice with Hyperpolarized 13C-SIRA. *Talanta* **2021**, *235*, 122812. https://doi.org/10.1016/j.talanta.2021.122812.

(20) Batel, M.; Däpp, A.; Hunkeler, A.; Meier, B. H.; Kozerke, S.; Ernst, M. Cross-Polarization for Dissolution Dynamic Nuclear Polarization. *Phys Chem Chem Phys* **2014**, *16* (39), 21407–21416. https://doi.org/10.1039/C4CP02696A.

(21) Bornet, A.; Melzi, R.; Perez Linde, A. J.; Hautle, P.; Van Den Brandt, B.; Jannin, S.; Bodenhausen, G. Boosting Dissolution Dynamic Nuclear Polarization by Cross Polarization. *J. Phys. Chem. Lett.* **2013**, *4* (1), 111–114. https://doi.org/10.1021/jz301781t.

(22) Dey, A.; Charrier, B.; Lemaitre, K.; Ribay, V.; Eshchenko, D.; Schnell, M.; Melzi, R.; Stern, Q.; Cousin, S. F.; Kempf, J. G.; Jannin, S.; Dumez, J.-N.; Giraudeau, P. Fine Optimization of a Dissolution Dynamic Nuclear Polarization Experimental Setting for $^{13}$ C NMR of Metabolic Samples. *Magn. Reson.* **2022**, *3* (2), 183–202. https://doi.org/10.5194/mr-3-183-2022.

(23) Ribay, V.; Dey, A.; Charrier, B.; Praud, C.; Mandral, J.; Dumez, J.-N.; Letertre, M. P. M.; Giraudeau, P. Hyperpolarized 13C NMR Spectroscopy of Urine Samples at Natural Abundance by Quantitative Dissolution Dynamic Nuclear Polarization. *Angew. Chem. Int. Ed.* **2023**, e202302110. https://doi.org/10.1002/anie.202302110.

(24) Bowen, S.; Hilty, C. Rapid Sample Injection for Hyperpolarized NMR Spectroscopy. *Phys. Chem. Chem. Phys.* **2010**, *12* (22), 5766. https://doi.org/10.1039/c002316g.

(25) Ceillier, M.; Cala, O.; El Daraï, T.; Cousin, S. F.; Stern, Q.; Guibert, S.; Elliott, S. J.; Bornet, A.; Vuichoud, B.; Milani, J.; Pages, C.; Eshchenko, D.; Kempf, J. G.; Jose, C.; Lambert, S. A.; Jannin, S. An Automated System for Fast Transfer and Injection of Hyperpolarized Solutions. *J. Magn. Reson. Open* **2021**, *8–9*, 100017. https://doi.org/10.1016/j.jmro.2021.100017.

(26) Joseph, D.; Sukumaran, S.; Chandra, K.; Pudakalakatti, S. M.; Dubey, A.; Singh, A.; Atreya, H. S. Rapid Nuclear Magnetic Resonance Data Acquisition with Improved Resolution and Sensitivity for High-throughput Metabolomic Analysis. *Magn. Reson. Chem.* **2021**, *59* (3), 300–314. https://doi.org/10.1002/mrc.5106.

(27) Pudakalakatti, S. M.; Dubey, A.; Jaipuria, G.; Shubhashree, U.; Adiga, S. K.; Moskau, D.; Atreya, H. S. A Fast NMR Method for Resonance Assignments: Application to Metabolomics. *J. Biomol. NMR* **2014**, *58* (3), 165–173. https://doi.org/10.1007/s10858-014-9814-6.

(28) Negroni, M.; Turhan, E.; Kress, T.; Ceillier, M.; Jannin, S.; Kurzbach, D. Frémy's Salt as a Low-Persistence Hyperpolarization Agent: Efficient Dynamic Nuclear Polarization Plus Rapid Radical Scavenging. *J. Am. Chem. Soc.* **2022**, *144* (45), 20680–20686. https://doi.org/10.1021/jacs.2c07960.

(29) Negroni, M.; Guarin, D.; Che, K.; Epasto, L. M.; Turhan, E.; Selimović, A.; Kozak, F.; Cousin, S.; Abergel, D.; Bodenhausen, G.; Kurzbach, D. Inversion of Hyperpolarized $^{13}$C NMR Signals through Cross-Correlated Cross-Relaxation in Dissolution DNP Experiments. *J. Phys. Chem. B* **2022**, *126* (24), 4599–4610. https://doi.org/10.1021/acs.jpcb.2c03375.

(30) Bornet, A.; Melzi, R.; Perez Linde, A. J.; Hautle, P.; van den Brandt, B.; Jannin, S.; Bodenhausen, G. Boosting Dissolution Dynamic Nuclear Polarization by Cross Polarization. *J. Phys. Chem. Lett.* **2013**, *4* (1), 111–114. https://doi.org/10.1021/jz301781t.

(31) Dey, A.; Charrier, B.; Martineau, E.; Deborde, C.; Gandriau, E.; Moing, A.; Jacob, D.; Eshchenko, D.; Schnell, M.; Melzi, R.; Kurzbach, D.; Ceillier, M.; Chappuis, Q.; Cousin, S. F.; Kempf, J. G.; Jannin, S.; Dumez, J.-N.; Giraudeau, P. Hyperpolarized NMR Metabolomics at Natural $^{13}$C Abundance. *Anal. Chem.* **2020**, *92* (22), 14867–14871. https://doi.org/10.1021/acs.analchem.0c03510.

(32) Bornet, A.; Pinon, A.; Jhajharia, A.; Baudin, M.; Ji, X.; Emsley, L.; Bodenhausen, G.; Ardenkjaer-Larsen, J. H.; Jannin, S. Microwave-Gated Dynamic Nuclear Polarization. *Phys. Chem. Chem. Phys.* **2016**, *18* (44), 30530–30535. https://doi.org/10.1039/C6CP05587G.